



Review paper

Effects of full displacement pile installation on the stress and deformation state of surrounding soil: review

Worku Firomsa Kabeta

Abstract: Several field and model tests have been conducted to investigate the impact of pile installation on bearing capacity. However, little is known about how piles behave during installation, how they interact with the surrounding soil, and how this affects sandy soil properties. This review paper investigates the effect of pile driving on surrounding sandy soil as it compacts sandy soil near to the pile. For this purpose, various related literature was studied based on the observation of the pile installation effect on earth pressure or lateral stress, relative density, and pore water pressure in the sandy soil. A change in the deformation and stress state of surrounding sandy soil due to pile driving was presented. The installation of fully displacement piles can lead to significant stresses and deformations in the surrounding sandy soil. This is one of the main causes of uncertainty in the design and analysis of pile foundations. According to this study, the sandy soil around the pile is compacted during pile driving, resulting in lateral and upward displacement. This leads to the densification effect of pile driving on loose sandy soil. Sandy soil improvement with driven piles depends on pile shape, installation method, and pile driving sequences. This study concludes that in addition to its advantages of transferring superstructure load to deep strata, the increased relative density of loose sand, the change in the horizontal stress, and the influence of compaction on the sandy soil parameters during pile driving should be considered during pile design and analysis.

Keywords: bearing capacity, driven pile, lateral stress, pore water pressure, soil improvement

1. Introduction

Loose sandy deposits should be improved to meet the sandy soil requirements of large infrastructural projects, reducing sandy soil settlements and structural deformations. Sandy soil densification may also result in a reduction of liquefaction risk in saturated sandy soils [1, 2]. There are many methods of deep sandy soil compaction, including dynamic compaction, vibro-flotation or vibro-driving, sand pile compaction, compaction grouting, compaction by blasting, and the pile compaction method. Steel, concrete, timber, or composite piles arranged in a grid can be used for the latter. The piles with different shapes, either constant with depth or tapered, can be installed in loose sand by driving, vibro-driving, cyclic jacking, or statically pushing in. Pile driving has unquestionably been favored among the various forms of pile installation due to its numerous advantages, including high bearing capacity, rapid construction speed, and suitability for a wide range of sandy soil conditions [2]. Due to noise and vibrations, their use in urban areas or near existing structures is, however, limited. Vibro-driving can reduce the force needed for installation decreasing the shaft friction. The pile base resistance could, however, increase during the vibro-driving process [3]. Depending on the soil grain-size characteristics, soil behavior, in situ soil density, pile spacing, and pile diameter, the installation process can result in measurable densification and an increase in lateral stress [4]. Recently developed technologies of cyclic jacking and pushed-in piles can overcome the difficulties related to noise and vibration level of previously described installation methods. The current knowledge about the effect of pile driving on the surrounding sandy soil is reviewed and presented in this study, which takes into account changes in stress state and displacement field, sandy soil density, and pore water pressure.

2. Effect of pile driving on the surrounding soil

The full displacement pile installation process can cause significant stress and deformation in the surrounding sandy soil. This is a key source of uncertainty in pile foundation analysis and design. A drive or jacking operation used to install a displacement pile generates changes in the sandy soil characteristics and stress-strain states that affect pile settlement and bearing capacity [5].

2.1. Effect on the stress and deformation state

During pile driving, the sandy soil is vertically and radially pushed out to allow the pile penetration. As a result, the final lateral stress will be quite different from the in-situ stress in the free field (Fig. 1). The pile installation method has a significant impact on the vertical capacity of the sandy soil due to the high level of energy induced on it during pile driving.

The entire stress field around the piles must be established to understand and model pile sandy soil-structure interaction, load-displacement response, group action, and time-



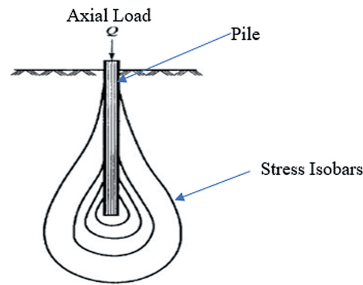


Fig. 1. Stress distribution near single pile [6]

dependent behavior. In comparison to bored piles, driven piles produce a pre-stressed sandy soil mass around the pile base, resulting in a stiffer pile base response. The mechanism of pile base penetration is similar to that of a cone penetration test, and the cone resistance is related to the ultimate base capacity [7].

As a result of the installation process, the sandy soil properties at the pile-sandy soil interface have also been observed to change. According to laboratory experiments by [8], the particle size distribution near the pile can be changed, reducing the interface friction angle at large deformations. The behavior of the sandy soil surrounding the pile during the pile installation is complex, and different laboratory tests on sandy soil properties, interface parameters, and experiments, including calibration chamber or centrifuge test, should be used to model the entire system [9–11].

The effects of different installation methods, jacking and impact driving, are investigated for three different initial relative densities of sand [9]. According to their findings, the sandy soil state depending on the method of installation (impact driving and pile jacking) varies significantly, and is also dependent on the sand initial density. The horizontal stress surrounding the pile increases with both impact driving and pile jacking. In jacked piles, however, the increase in horizontal stress is much greater than in impact-driven piles. Henke and Grabe [10] found that in a moderate-density sample of sand having relative density of 51–55%, the external horizontal stress in the vicinity of the pile tip is much lower after impact driving than jacking. Higher vertical stress near the pile tip is expected after jacking than after impact driving. However, the degree of sandy soil densification is higher after impact driving than after jacking, especially near the top of the pile. As a result of impact driving, the horizontal stress in the area below the pile tip increases. Improved sandy soil strength is the result of the combined effects of increased stress and decreased void ratio (sandy soil compaction). The magnitude of the peak horizontal stress increases as the initial relative density of sand increases. Jacked piles are also prone to sandy soil arching more than impact-driven piles. During pile jacking, stress changes in the sandy soil are significant near the pile, but they also extend a significant radial distance. Model tests and field measurements have been conducted during pile installation with pressure cells in the sandy soil mass [3, 11].

Stress measurements are frequently taken in the field using a neighboring whose stiffness alters the stress field beneath the sandy soil. To quantify this inaccuracy, precise stresses

measurements caused by a single pile installation in laboratory conditions are required. Jacked pile experimental results [12] for sand show that with increasing h/R , the radial effective stress decreases, where h is the distance above the pile tip and R is the pile radius. During the jacked installation of a cylindrical pile in dry sand in a centrifuge, D'Arezzo et al. [13] used null gauges to measure horizontal stress changes. Stress is measured using both an adjacent pre-installed square pile and in-sandy soil sensors. The normalized depth of the pile tip (h/R) and the ratio of the increment of horizontal stress ($\Delta\sigma_h$) to the pile base stress (q_b) were calculated. As a result, the maximum horizontal stress increment at 9D from the pile is 0.5 percent of the base resistance, indicating that horizontal stress decreases with increasing distance from the pile. The maximum changes in horizontal pressure occur when the pile tip is slightly above sensor level; the distance below the pile tip at which the maximum stress is detected is greater for shallower depths of penetration. Jardine et al. [14] obtained similar results at the same distance during the installation of a cylindrical pile in a calibration chamber.

Hughes and Robertson et al. [15] discovered that when a cone penetration test (CPT) probe penetrates sand, a highly stressed, rigid ring of sand forms around the tip. During pile penetration into sandy soil, there is a friction between loose sand and the pile. A thick cylinder of sand encircles the loosened sands and prevents the formation of complete lateral earth pressure on the pile through arching [16, 17]. Sandy soil arching is a pressure redistribution phenomenon caused by relative movement between adjacent portions of the sandy soil (Fig. 2). When sandy soil interacts with structural elements, such as sandy soil-pile interactions, it is a common occurrence. Physical model of driven displacement piles can also be created using the full-displacement probe. After installation, the radial stress (σ'_r) acting around the pile at any depth (z), was found to vary with cone penetration test resistance, which reflects stiffness of sand and conditions, and to decrease as the pile installed and the relative depth above the tip increased. There was also a small reliance on

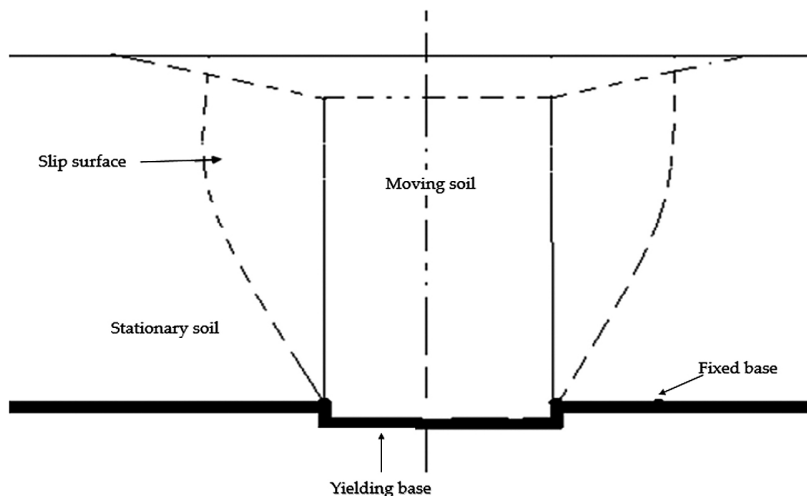


Fig. 2. Stress redistribution caused by arching [19]

the effective vertical stress (σ'_z). Nguyen et al. [18] has proposed equivalent stiffness-based load transfer model as an effective tool for analyzing behaviors of the open-ended pile in considering the soil plugging effect. This model aims to replace the sum of unit stiffness's corresponding with external and internal unit skin frictions in the basic differential equation of load transfer by a weighted average of equivalent unit stiffness's using a dual approach of equivalent replacement.

Bond and Jardine et al. [20] proposed the equation (1) for radial stress expression for the design of cylindrical piles driven in sands.

$$(2.1) \quad \sigma'_{rc} = f(z) = 0.029q_c \left(\frac{\sigma'_{zo}}{P_A} \right)^{0.13} \left(\frac{h}{R} \right)^{-0.38}$$

In which P_A is the atmospheric pressure. The relative depth above or below piles tip (h/R) and cone tip resistance (q_c) variables have significant effects, but a change effective vertical stress (σ'_z) only results in a 35% change in the radial stress (σ'_r).

The stresses in the pile vicinity fluctuate dramatically as the distance between the pile axis and the radial distance increases, and as the distance between the pile tip and the top of the pile increases, according to all of the trials. When these data are combined with the field trends captured in the above equation (2.1), it appears that radial stress (σ'_r) may be stabilized for fluctuations in free-field vertical stress σ'_z and local cone tip resistance (q_c), and represented by 2D functions of the form.

$$(2.2) \quad \frac{(\sigma'/q_c)}{(\sigma'_{zo}/P_A)^{0.13}} = f\left(\frac{h}{R}, \frac{r}{H}\right)$$

Yang et al. [8] performed experimental investigations and three computational evaluations of stresses created around piles penetrating into sand. The cylindrical stresses surrounding piles intruding into normally consolidated quartz sand were investigated using a combination of three experimental studies and three numerical analyses.

The interpretation summarizes predicted and measurement made at points between 10 and 550 kPa of the actual initial stress between the relaxed and stressed states, which are related to stresses with Cone penetration test and dimensionless ratio of vertical stress $(\sigma'_{zo}/P_A)^{0.13}$. The dimensionless spatial coordinates ($h = R$, $r = R$), where the top of the pile is the origin of the coordinates, represent the final states and ($h = R_p$, $r = R_p$) represent the stresses around the exposed pile at moderate radial distances.

Jardine et al. [14] interpreted stress measurements and presented the distribution of circumferential or vertical stress and radial stress as a function of distance to the penetrating pile in dense sand. They jacked up instrumented model piles in the calibration chamber with sandy soil mass equipped with stress sensors. Emphasis was placed on the effective radial stresses occurring around the axes of the columns, but circumferential and vertical stresses were also taken into account. They interpreted detailed stress measurements taken on and around closed-ended model displacement piles in pressurized silica sand. The stresses that develop at any point are primarily determined by CPT tip resistance and spatial position



relative to the pile tip (h/R and r/R), as expressed by:

$$(2.3) \quad \frac{\sigma'}{q_c} = f\left(\frac{h}{R}, \frac{r}{H}\right)$$

where h/R is the (positive) relative height above or (negative) relative depth below the pile tip, and r/R is the relative radius from the pile axis.

The sandy soil stresses vary spatially in relation to the pile tip location. The stress measurements performed by Jardine et al. [14] revealed that sandy soil stresses developed during installation were directly correlated with local q_c values; normalization by q_c reduced the impact of test arrangement variations. Although the datasets have similar initial σ'_{rs}/q_c maxima as the pile tip passes and fall to similar final low σ'_{rs}/q_c ratios (σ'_{rs} is stationary radial stress), the decay curves applied between these limits converge better when plotted against h/R than when plotted against the number of cycles (N), indicating a closer correlation with relative pile tip depth than with the number of cycles. On-pile measurements show that doubling N did not result in steeper radial stress reductions for fixed h/R ratios. Sandy soil mass stresses were unaffected by the number of jacking cycles. These characteristics, on the other hand, may be more important at the pile/sandy soil interface, during dynamic installation, and over extended periods of time.

During both the penetration and pause stages, stress distributions established in the sandy soil below and to either side of the tip level stress are roughly spherically symmetrical, though there are minor differences between the stress decay curves established on vertically and horizontally projected distributions.

Close to the pile tip, very steep stress gradients apply, with triaxial conditions dominating directly under the tip, where $\sigma'_z = \sigma'_1 \approx q_c$ and $\sigma'_{rm} = \sigma'_{\theta m} \approx q_c/Kp$, in which Kp is Rankine coefficient of passive earth pressure, σ'_1 is major principal effective stress, $\sigma'_{\theta m}$ is moving circumferential stress, and σ'_{rm} is moving radial stress.

After installation, the radial stress level reaches peaks at normalized around significant radial distances $r/R = 3$, which are roughly double those operating on the shaft ($r/R = 1$). At $r/R > 3$, σ'_{rm}/q_c declines consistently with h/R for any given r/R and all radial stresses decompose with radius. Circumferential stresses vary at $1 < r/R < 5$ range, according to the radial equations of equilibrium and $\sigma'_{rs} < \sigma'_{\theta m}$ at $1 < r/R < 3$ once installed. Here, one should notice that the maximum radial stress is not on the pile shaft, but at some distance. In low to medium density quartz sand, Lehane et al. [12] took extensive measurements of the effective stresses generated during installation, equalization, and load testing of displacement piles. They demonstrated that the stresses that develop at any given sandy soil horizon are strongly influenced by the horizon's distance from the pile tip as well as the sandy soil's initial state. As each jacking stage was started, the effective radial stresses (σ'_r) rised by 5 to 20 kPa, causing the stationary profiles of σ'_r , known as σ'_{rs} , to separate from those recorded during the pile was moving. The long-term, fully equalized values (σ'_{rc}) for a pile that has penetrated to the same tip depth but no further are the same as the stationary radial stresses recorded during installation pause periods (σ'_{rs}), where σ'_{rc} is the radial effective stress after equalization and σ'_{rs} is the stationary radial effective stress.



Another study on the change in horizontal stress during pile driving were conducted by D'Arezzo et al. [13]. Null-gauges were used to measure horizontal stress changes during the jacked installation of a cylindrical pile in dry sand. They used an adjacent pre-installed square pile and in-sandy soil sensors to measure stress, and then compared the centrifuge results to the radial stress distribution estimated using traditional methods. Their findings show that when the pile is at an equal distance between the pile null gauges and the sandy soil null gauges, the pile experiences higher stresses due to its stiffness. For the determination of stress state near pile base [21] conducted field tests on piles equipped with surface stress transducers and discovered that severe stress fluctuations occur during sand penetration, particularly around the tips.

Beijer Lundberg et al. [22] conducted a series of geotechnical centrifuge tests of displacement pile installation in sand with various initial relative densities. The stress measurements included horizontal and axial contact stresses. The deformation measurements were displayed as displacement trajectories, with incremental stresses and sandy soil displacements analyzed. The effect of load cycles and the influence of initial relative density were the focus of the measurement's interpretation. During pile installation and removal, the initial relative density was shown to have a significant impact on the horizontal contact stress. The horizontal displacement measurements revealed a similar impact, with denser sandy soil samples exhibiting higher horizontal displacement. It was discovered that the sandy soil compaction during cyclic loading shows in decreased horizontal contact stress. Dense, medium dense and loose sand with initial relative densities 0.4, 0.6 and 0.8 respectively were tested. The installation effects are strongly influenced by the relative density of the sandy soil at the start of the experiment, according to the results. The measurements were compared to numerical models that produced similar results.

Lehane et al. [21] also used a drum centrifuge to test model piles in normally consolidated sand to see how the method of pile installation, level of stress, and aspect ratio of pile affected the increase in lateral stress on the pile while load testing. They consider pile aspect ratio (elongation) in the model tests as 1 for 14 model piles, 2 for two model piles and 6 for other two model piles. The ratios of lateral stress increases (the ratio of lateral stress in pseudo-dynamic mode to jacked mode) measured during installation for $h/D = 3$ is higher than for $h/D = 6$, where D is pile breadth. The difference between pseudo-dynamic and jacking installation mode is that piles area installed in a sequence of jacking strokes during jacked installation. For each stroke, the piles were pushed at 0.2 mm/s for 2 mm, then extracted at 0.005 mm/s until the pile head load was zero. During pseudo-dynamic installation, the piles were installed in a series of 2 mm downward jacking increments at 0.2 mm/s, followed by 1.5 mm extraction at 0.2 mm/s. Furthermore, due to sandy soil compaction near the pile toe, base resistance increases with the number of cycles applied, whereas shaft load decreases with the number of cycles applied due to sandy soil densification next to the pile shaft [20].

Fig. 3 describes the effect of pile installation mode on lateral stress for both stationary and moving pile conditions. For the same type of installation method, lateral stresses when the pile is moving are greater than the lateral stresses when the pile is stationary [21]. They also discovered that the magnitude of lateral stress decreases as the distance between the pile tip and the pile diameter (h/D) increases for both methods of installation.



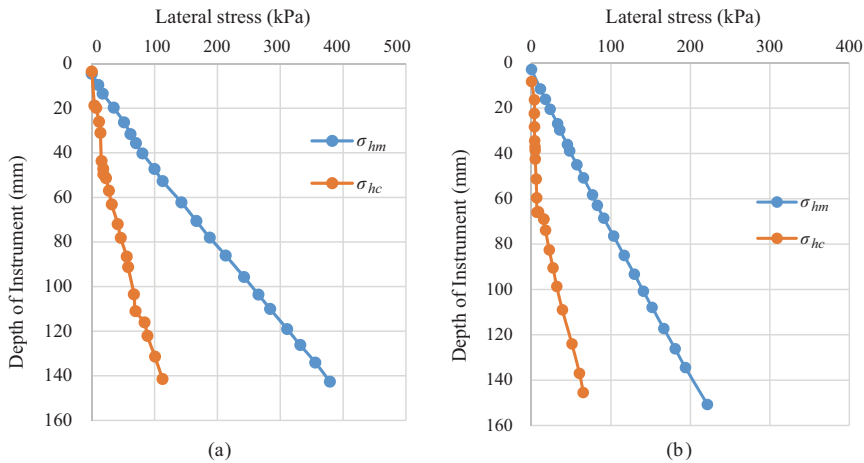


Fig. 3. Lateral stresses (a) jacking installation; (b) installation by pseudo-dynamic [21], σ_{hc} is lateral stresses when pile is stationary and σ_{hm} is lateral stresses when pile is moving

Different measurement techniques are used to measure the deformation field around installed model piles. Otani et al. [23] investigated the deformation of sand surrounding a laterally loaded pile using X-ray computed tomography. Due to the high cost of CT scanners, it has limited application in geotechnical engineering. Particle image velocimetry (PIV), a cost-effective, accurate and full-field image correlation approach has been employed in geotechnical engineering since the invention of digital image process [24]. In geotechnical research laboratories, PIV techniques have been used to measure sandy soil deformations around a driven pile in sand in geotechnical models [26–28].

According to study by White et al. [25], PIV is a velocimetry method that tracks textured particles in a series of images. Image processing algorithms have been written to apply the PIV principle to surface images. The resulting software is capable of tracking the movement of natural sand or sandy soil to an accuracy of 1/15 pixel. The combination of digital imaging and PIV analysis makes it possible to calculate strain fields consisting of thousands of displacement vectors with greater accuracy than the averaging method. Beijer-Lundberg [27] have also used PIV program to analyze stress and deformation measurements using experimental tests. The effects of initial relative density and load cycles were the focus of the measurements' interpretation. The horizontal displacement measurements revealed a similar effect on soil density, with denser sandy soil samples exhibiting more horizontal displacement. In the stress and deformation measurements, the effect of incremental installation was examined, and it was discovered that compaction of the sandy soil during cyclic loading results in lower horizontal contact stress.

Numerical simulation of pile installation conducted by [28] compares experimental results with centrifuge tests. Both results show the development of large effective vertical stress below the pile base and porosity change near the pile shaft, also differences with the experimental results are found.

Figure 4 shows the displacement contours after installation and displacement paths. In Fig. 4a, the boundary without any displacements is shown as a thick dark line. These influence zones show where the sandy soil is moved during the installation. According to the measurements, a pile model should at the very least include the boundaries of no displacements. The sandy soil sample container should also be wider, according to these measurements. Fig. 4b also shows the displacement path for loose sandy soil and dense sandy soil, showing that the initial density of the sandy soil sample has a relatively large effect, with the dense sandy soil sample experiencing more heaving vertical displacement than the loose sandy soil sample.

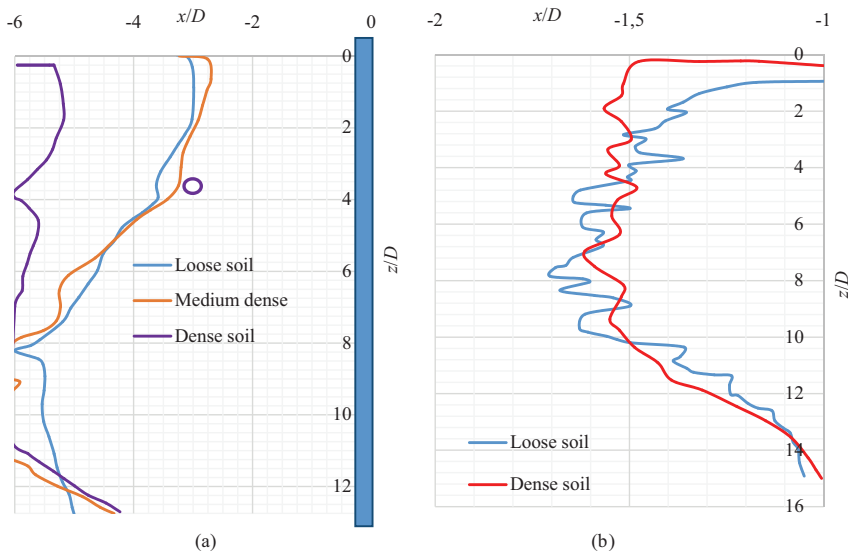


Fig. 4. Displacement contours and paths (a) displacement contours and (b) vertical arrays of displacement path for typical location [27]

2.2. Effect on pore water pressure

Because of sandy soil compaction, pore water pressure rises during pile driving in loose sands and sandy silts, causing a reduction in effective sandy soil strength. The shear strength (τ) of saturated $C - \phi$ sandy soil is defined by Mohr Coulomb criteria as cited in [29]:

$$(2.4) \quad \tau = C + \sigma'_n \tan \phi = C + (\sigma_n - U) \tan \phi$$

where C is cohesion parameter, σ_n is total normal stress, ϕ is internal friction angle, σ'_n is effective normal stress and U is pore water pressure and can be determined as,

$$(2.5) \quad U = \gamma_w z$$

where z is depth from water table level to pile tip and γ_w is unit weight of water.

Numerous studies have tried to model the pore water response to pile installation or even other construction vibrations in the near-field analytically [5, 30, 31]. The initial stresses in the sandy soil before the pile is driven are the horizontal effective stress (σ'_3), the vertical effective stress (σ'_1), and the pore pressure (U).

The horizontal effective stress (σ'_3), vertical effective stress (σ'_1), and pore pressure (u_0) are the initial stresses in the sandy soil before the pile is driven. Vertical and horizontal stresses are also the principal stresses. Because the horizontal strain in a natural deposit is zero, σ'_1 equals $K_0\sigma'_3$ where K_0 is the coefficient at rest earth pressure [32].

Radial stress becomes the most critical stress within the failure zone during pile driving. The maximum excess pore pressure (Δu_m) that results will be made up of two parts, one from the change in total ambient stress ($\Delta\sigma_3$), and the other from shearing, as follows [32]:

$$(2.6) \quad \Delta u_a = (1 - K_o) \sigma'_1$$

$$(2.7) \quad \Delta u_s = \left(\frac{\Delta u}{p} \right)_m \sigma'_1$$

where p is the consolidation pressure, Δu_a is the change in pore water pressure from total ambient pressure, Δu_s the change in pore water pressure from shearing and $\left(\frac{\Delta u}{p} \right)_m$ the maximum pore pressure ratio. Hence,

$$(2.8) \quad \Delta u_m = \Delta u_a + \Delta u_s = \left[(1 - K_o) + \left(\frac{\Delta u}{p} \right)_m \right] \sigma'_1$$

The pore-pressure ratio $\left(\frac{\Delta u}{p} \right)_m$ rises with the applied stress differential, reaches its maximum $\left(\frac{\Delta u}{p} \right)_m$, and then remains constant when a specific strain is reached [32].

The extra pore water pressure generated below the pile toe while driving in fine sandy soil was monitored [33], and the magnitude level of applied force and the strength level of sandy soil material are the conditions affecting the level of excess pore water pressure. If these two parameters are at high level, the excess pore water pressure is considered to increase to the point of destruction of sandy soil texture, and then produce the liquefaction phenomenon. A high-pressure zone of excess pore water was forming under the pile toe. This high-pressure zone operated as a barrier to pile driving, making further pile insertion impossible. The pile toe generated excessive pore water pressure, which spread throughout the surrounding area, with this pressure being transferred to the pile toe of the pre-driven pile.

At various distances from driven piles, variations in pore water pressures were measured in sandy and clayey sandy soil layers by Hwang et al. [34]. To control the response of sandy soil pore water pressure caused by pile driving, they used electrical piezometers. The pore water pressure of sandy soil positioned at a radial distance of $3D$ from the center of the pile began to climb when the pile tip advanced to an elevation of 4 to $7D$ (D is the pile diameter) above the piezometer site, and reached its maximum value when the pile tip passed $4D$ below the piezometer location. At a distance of $3D$ from the pile's center, the

extra pore water pressure in a sandy layer at 6 m below ground reached 1.5 times the effective overburden pressure, resulting in liquefaction conditions.

According to Fattah and Mustafa [35], twelve experiments with piles installed by overdriving were carried out on a fine sandy soil of medium density with a relative density of 60%. The changes in excess pore water pressure were measured at both the pile tip and the pile middle. The study reveals that pile slenderness ratio, machine operation frequency, and sandy soil permeability are the parameters that influence the formation of extra pore water pressure. The excess pore water pressure generated during operation, however, was found to be less than 20% of the initial hydrostatic pressure in all cases.

As the pile group installation is considered [32], the pore pressures due to the driving of each pile are quite easily discernible. For piezometers placed close to the pile, the maximum pore pressure is recorded about 20 minutes after the pile reaches the level of the piezometer tip. There is a slight effect of pore pressure redistribution from regions of high pressures to regions of low pressures for piezometers located further away from the pile.

Pore-water pressures were measured by inserting two piezometers at 9 and 18 meters below the ground surface during the inspection of piling activities [36]. Prior to the piling operations, readings from all piezometer were taken on a regular basis, at least once a day. As pile driving got closer, the piezometers readings were taken before and after each pile were driven. A significant increase in pore water pressure was generated at both the shallow and deep piezometers during pile section drive into very dense sand and gravel.

The amount of excess pore water induced during pile driving can be reduced by applying additional drains installed in the timber piles [37]. The extra pore pressure generated by 48 test piles with drains and 13 test piles without drains was measured. When the drain was used, the data showed that excess pore pressure was reduced by at least 50%. Furthermore, the procedure proved much less expensive than other methods for dealing with dangerously high pore water pressures caused by piling in similar sandy soils. Pestana et al. [38] performed a geotechnical site investigation and a site control testing to measure horizontal loads and pore water pressure at three radial distances from large closed piles. Their findings show that pile driving causes significant excess pore pressures, which are related to the distance from the pile wall. Due to the excessive pore pressure generated by the pile installation, the initial effective vertical stress of the sandy soil is slightly exceeded within one pile diameter. The generated excess pore pressure decreased as distance from the pile–sandy soil interface ($1/R^2$, where R is the distance from the pile's center) increased. These pore pressures dissipate over time, and sandy soils more than one diameter away from the pile wall achieve 80% consolidation between 50 and 80 days. Initial inclinometer measurements of outward radial deformations were very close to predictions based on cylindrical cavity expansion theory. Lateral deflection measurements show a return to the pile as the excess pore pressure dissipates, with a decreasing magnitude as the distance from the pile wall increases.

2.3. Effect on density/compaction of soil

There is the densification due driving pile on sandy soil. As a result, sandy soil around the pile is compacted and lateral and upward displacement will occur. Several scholars and practicing engineers [2, 34, 39–41] have described the improved conditions that resulted



from pile driving. The volume and shape of the pile, as well as the method of drive, determine the amount of this compacted area and the characteristics of the sandy soil within it.

Depending on the grain size characteristics of the sandy soil, on-site sandy soil density, pile spacing, and pile diameter, the installation process can cause visible compaction and an increase in lateral stress [40]. It is well known that loose, clean, granular sandy soils contract when displacement piles are installed [16]. When piles are installed in loose sand, some compaction occurs up to 3.5 to 6 pile diameters away from the pile shaft [42]. Szechy [43] also found that the void ratio decreased by around 5% near the lower half of driven piles. Unfortunately, few studies have been conducted since then on the extent and distribution of compaction around displacement piles.

The development of displacements around a full displacement pile causes loose sand to compact. The degree of sand compaction induced by driving has been related to bearing capacity improvement for pile [42]. Previous bearing capacity theories were mainly founded on the assumption that the sandy soil conditions did not change as the pile was driven. However, pile driving not only increases the relative density of loose sand but also the horizontal stress and the influence of compaction on the sandy soil parameters cannot be ignored. The compaction increase caused by pile driving in loose sands can be related to the shift in the internal friction angle of sand and factored into pile ultimate bearing capacity estimates.

Meyerhof [42] examined the installation of a driven pile, resulting in compaction and a rise in the major stress ratio. He measured the width of the compacted zone around a single driven pile, and found that it was around 6 to 8 times the pile width. In model pile testing, Kishida [44] discovered that the distribution of displacement stresses caused by sand displacement as a result of pile driving was proportional to the width of the compacted zone. Based on their findings, the author determined that the width of this zone as $b = 7D$, as shown in Fig. 5.

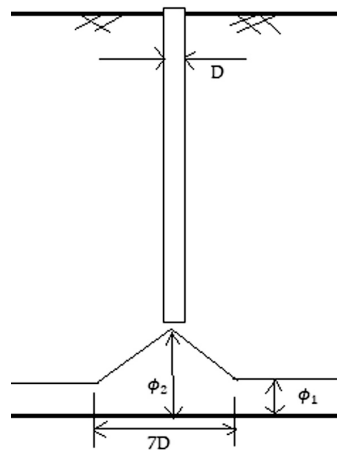


Fig. 5. Effect on friction angle (ϕ) [44]

Kishida [44] assumed that the internal friction angle changes linearly with distance from the pile (where $\phi = \phi_2$) to a radius of around 3.5 times the pile diameter (where $\phi = \phi_1$) in the compacted zone thus established. In the sand, the link between ϕ_1 and ϕ_2 can be stated [42, 44] as:

$$(2.9) \quad \phi_2 = \frac{\phi_1 + 40^\circ}{2}$$

where ϕ_1 – initial value friction angle, ϕ_2 – frictional angle after pile driving.

2.4. Compaction control tests

The quality of sandy soil compaction is verified through in-situ testing. The standard penetration test (SPT) performed between driven displacement piles [39] confirmed the increase in the number of standard penetration blows. Stuedlein et al. [41] demonstrated a test program for driven piles for sandy soil densification in silty sands and potentially liquefiable sands. Cone penetration tests revealed that as pile spacing was reduced, the resistance of the cone tip increased significantly. For $5D$ -spaced piles, the measured cone resistance nearly doubled, doubled to tripled for $4D$ -spaced piles, tripled for $3D$ -spaced piles, and resulted in rig-push refusal for $2D$ -spaced piles (as D is pile diameter). However, after about 8 months, the measured cone penetration resistance in all of the treated sandy soils decreased within much of the treated depths. These tests also revealed that cone tip penetration resistance can be reduced over time between 10 days and 255 days from the compaction works, and that the pile spacing appears to be the cause of these reductions. The reduction is most likely due to the relaxation of horizontal stresses at constant relative density, similar to how horizontal stresses are reduced after roller-type compaction [45]. These tests also confirmed the important effect, of drainage conditions during the timber pile driving. Some piles were equipped with drainage tapes along the pile shaft to reduce extra pore water pressure mobilized while pile driving and to improve the compaction effect. The long-term increase in cone resistance due to compaction with timber piles is two times higher for piles with installed drains compared to typical tapered piles [41].

Sandy soil compacted with timber piles driven in New Zealand was analyzed using CPT data [46]. Accordingly, the sandy soil density and cone tip resistance (q_c) consistently increase and the void ratio reduces throughout the sandy soil profile. The void ratio decreases in the range of 0.1–0.2 and the sandy soil density increases by about 50–100 kg/m³. The amount of increment in q_c is about 1–3 MPa in silty sand.

Cone penetration tests (CPTs) have been used by [47–49] to characterize the subsurface soil conditions and measure the load distribution along the length of the test piles and skin friction and end-bearing capacity using strain gauges. All the test piles were instrumented with vibrating wire strain gauges to measure the load distribution along the length of the test piles and measure the skin friction and end-bearing capacity, separately

Marchetti Dilatometer test (DMT) have been conducted in addition to CPT tests to investigate the impact of pile installation on the surrounding sandy soil by Munro [50], Peiffer et al. [51] and Van Impe [52]. The findings of their research demonstrate that



horizontal stress increases due to pile installation, which is dependent on the sandy soils over consolidation ratio (OCR), sandy soil type, dilatant character, and, most importantly, installation details. Both the improved panels and the natural homogeneous sandy soil properties in the Piezocone (CPTU) and seismic dilatometer (SDMT) tests [53] indicate good agreement in the geotechnical site characterization. In comparison to the results obtained from CPTU data, the increase in DMT parameters after treatment was more pronounced. The horizontal stress index (K_D) increased by 48–53%, constrained modulus (M) by 80–87%, and stress-normalized cone resistance (qt) by 30–35%, proving that DMT is more sensitive to increases in horizontal stress.

Furthermore, after treatment, a significant increase in K_0 and (M/qt) was discovered using a combination of DMT and CPTU tests, indicating that the piers can be used to mitigate liquefaction and increase lateral sandy soil stress. Hence, DMT tests can be considered as an efficient tool for deep sandy soil compaction control as they include both an increase in lateral stress and sandy soil constrained modulus [54]. The compaction criterion based on deformation modulus (Young's modulus, E) seems to include most of beneficial effects of deep sandy soil improvement.

3. Factors affecting soil improvement with driven piles

Pile spacing and pile-to-sandy soil area ratio are the most critical parameters for sandy soil improvement. Barounis and Philpot [46] elaborated a special design chart for sandy soil compaction with driven piles concerning initial sandy soil density, target sandy soil density, pile number, diameter and spacing. The relationship between the subsequent change in sandy soil densities and the pile-to-sandy soil area ratio is essentially linear. To achieve the necessary increase in density, larger diameter piles and a larger number of piles will be required as the difference between the original and goal sandy soil density grows. The chart also calculates the number of piles needed to achieve the desired density increase.

3.1. Effect of pile shape on bearing capacity

Driven displacement piles of various materials and forms have been utilized as compaction piles all over the world to improve ground conditions [53] and mitigate liquefaction risk [55].

The study by Lobo-Guerrero and Vallejo [56] and Lv et al. [57] shows that there is significant impact of pile shape on pile driving performance and densification of the surrounding sandy soil. They simulate piles of various shapes (flat tip, open pile, triangular tip) being driven into uniform crushable sandy soil that has been compacted using the Discrete Element Method (DEM). According to the DEM, the driven pile design has a substantial impact on particle crushing development and penetration resistance.

When a flat-ended pile was compared to a triangular-tipped pile, the flat-ended pile had the highest penetration resistance and caused the most crushing of the circular particles in its vicinity. The pile with the triangular tip had the least amount of grain crushing and



had the lowest penetration resistance. A few studies have conducted field tests to examine the shape of the pile in terms of bearing capacity and drivability [57–59]. Ghazavi [58] determined the drivability of tapered and cylindrical piles, as well as the ground vibrations induced in the surrounding area. The tapered pile had greater displacement and velocity than the cylindrical pile, and it performed better and had a greater effect on pile penetration and cost savings by increasing residual set per blow and velocity. This shows that pile shape and geometry have a direct effect on ground vibrations during driving.

One of the most promising shapes is the tapered pile, where the pile diameter is decreases with depth. They can be made of steel, concrete, or wood, or be produced from composite materials. Driven timber piles widely used for sub sandy soil improvement are the traditional example of tapered piles. The timber compaction piles were driven into the ground in order to improve the site's geotechnical performance with density and stiffness [46].

Because of their high bearing capacity, tapered piles have been increasingly popular in recent years [60]. Field and model experiments [61], theoretical studies [62], and numerical analysis [63] have all been used to explore the bearing capacity of tapered piles. Sakr and Naggat [64] have published field-testing results, and they reported that cylindrical piles with the same embedded depth and average diameter have a smaller total capacity than tapered piles.

Instrumented field testing [55] and analytical approaches developed to predict the behavior of tapered piles [65] have also helped to advance this knowledge.

In sandy soils, tapered piles can provide a stiffer axial response and a capacity increase of 200–250%, and reduced construction costs by 50% when compared with cylindrical piles of the same mean radius and volume [66].

3.2. Effect of pile driving sequence

It has long been known that the order in which displacement piles are installed in a group affects the driving resistance and pile capacity [16]. Reduced pile spacing resulted in significant increases in pile capacity, depending on the installation sequence. Quantifying the impact of pile installation sequence on pile capacity helps determine pile foundation as-built capacities and construction viability when reasonably close spacing is required. Due to the densification that occurs when the sandy soil void volume is filled with the volume of the piles, the installation sequence can affect their drivability in contractive sandy soils [67]. In dilative sandy soil, this effect could even stop the driving process.

In a deep sand deposit in Dunkirk, north France, Chow [68] investigated the stress interactions between two nearby piles. The influence of radial effective stress and changes in shear stress caused due to pile installation of a nearby pile on load-carrying capability was investigated. Model pile was used to measure the change in effective stress due to the construction of another pile at 4.5 diameters. According to the results of his study, the installation of adjacent piles increased the radial effective stresses, resulting in an increase in capacity of the shaft during the loading process. The development of these large stresses is associated with sand displacement and high stresses around penetration pile tips.



The pile group response is influenced by the installation sequence as well. The installation order is a critical factor influencing the pile group affect because local pile responses differ from those of the others in the group. When pile driving begins in the center of the pile group, the behavior is different from that when pile driving begins on the perimeter. The study on the sequence of pile installation effects in silica sand [69] shows that if the central pile is installed first, then the adjacent piles, the sandy soil mass surrounding the central pile will be densely packed as a result of the adjacent piles being installed first. When the central pile is installed first, however, the mobilized shaft friction is the lowest.

4. Summary and discussions

Table 1 shows the summary of studies related to the pile installation effects. The observation of the pile installation effect on earth pressure or lateral stress, relative density, and pore water pressure in the sandy soil is summarized.

Table 1. Summary of related literatures on the effect of pile installations

Pile installation effects on	Author	Objective of the study	Concluding remark
Stress and deformation state	Lehane et al. [12]	To measure effective stresses developed during the installation, equalization, and load testing of displacement piles	Stresses developed at any given sandy soil horizon depend on the distance of that horizon from the pile tip and initial sandy soil state
	Fan et al. [9]	To study the effect of pile installation on the initial stiffness and lateral capacity of pile	Impact-driven piles have significantly higher initial stiffness and lateral capacity than jacked piles. The effect of installation methods on the lateral response is also influenced by the initial sandy soil density, driving distance, pile geometry, stress level, and load eccentricity
	D'Arezzo et al. [13], Yang et al. [8], Jardine et al. [14], Beijer Lundberg et al. [22]	To measure horizontal stress changes during the jacked installation	Stress is measured using both an adjacent pre-installed square pile and in-sandy soil sensors. The maximum changes in horizontal pressure occur when the pile tip is slightly above sensor level; the distance below the pile tip at which the maximum stress is detected is greater for shallower depths of penetration



Table 1 [cont.]

Pile installation effects on	Author	Objective of the study	Concluding remark
Density and compaction of sandy soil	Homayoun Rooz and Hamidi [2], Hwang et al. [34], Nataraja and Cook [39], Siegel et al. [40], Stuedlein et al. [41], Meyerhof [42], Szechy [43], Kishida [44],	To examine change in sandy soil density and compaction during pile driving	Pile driving in sandy soil increase sandy soil density and compact the sandy soil surrounding the pile. Horizontal stress increases due to pile installation.
Pile shape and Pile driving sequence	Amoroso et al. [53], Stuedlein et al. [55], Lobo-Guerrero and Vallejo [56], Lv et al. [57], Ghazavi [58], Naggar et al. [59], Leo et al. [60], Yang et al. [61], Sakr et al. [62], Butterfield and Banerjee [63], Hesham El Naggar [64], El Naggar [65], Sherstnev et al. [66]	To examine the effect of pile shape on pile driving performance and densification of the surrounding sandy soil	The tapered pile had greater displacement and velocity than the cylindrical pile, and it performed better and had a greater effect on pile penetration and cost savings by increasing residual set per blow and velocity. Tapered piles can provide a stiffer axial response and a capacity increase of and reduce construction costs.
	Robinsky and Morrison [16], Chow [68], Francis et al. [69]	To determine the impact of pile installation sequence on sandy soil compaction and pile capacity	The installation sequence can affect their drivability of pile and the density of sandy soil.

5. Conclusions

This study reviews the effects of pile installation in improving the sandy soil. Special considerations were given on the change in lateral stress, relative density, and pore water pressure in the sandy soil during pile driving. Fully displacement piles can cause significant stresses and deformations in the sandy soil surrounding them. This is one of the main causes of uncertainty in the design and analysis of pile foundations. During driving pile in loose sands and sandy silts, pore water pressure rises due to sandy soil compaction. High compressive stresses arise in the adjacent sandy soils during the driving of high displacement piles, resulting in a buildup of large effective lateral stresses. The compaction of the sandy soil mass surrounding a pile increases its bearing capacity. As a result, the driven pile can be utilized as a sandy soil compactor to enhance the sandy soil surrounding the pile. The degree of sand compaction caused by driving the pile was related to the increase in bearing capacity of the driven pile in sand. The shape of driven piles has a significant impact on the degree of ground improvement achieved, revealing that driven tapered piles are more effective in densifying the ground than straight cylindrical ones. The spacing of displacement piles and the installation sequence affect their drivability. Unfortunately, few studies have been conducted since then on the extent and distribution of compaction around displacement piles. As the effect of pile shape on stress and deformation state is not well known in the case of tapered piles, the sandy soil deformation and stress fields around constant diameter piles and tapered piles will be studied in a series of tests planned in the centrifuge at Gustave Eiffel University in Nantes within the Geolab project. The bearing capacity of constant diameter piles and tapered piles will be compared for the installation mode with driving and jacking. The sandy soil deformation fields will be estimated using the PIV technique.

References

- [1] A. Janalizadeh, A. Zahmatkesh, "Lateral response of pile foundations in liquefiable soils", *Journal of Rock Mechanics and Geotechnical Engineering*, 2015, vol. 7, no. 5, pp. 532–539; DOI: [10.1016/j.jrmge.2015.05.001](https://doi.org/10.1016/j.jrmge.2015.05.001).
- [2] A.F.H. Rooz, A. Hamidi, "A numerical model for continuous impact pile driving using ALE adaptive mesh method", *Soil Dynamics and Earthquake Engineering*, 2019, vol. 118, pp. 134–143; DOI: [10.1016/j.soildyn.2018.12.014](https://doi.org/10.1016/j.soildyn.2018.12.014).
- [3] S. Moriyasu, S. Kobayashi, T. Matsumoto, "Experimental study on friction fatigue of vibratory driven piles by in situ model tests", *Soils and Foundations*, 2018, vol. 58, no. 4, pp. 853–865; DOI: [10.1016/j.sandf.2018.03.010](https://doi.org/10.1016/j.sandf.2018.03.010).
- [4] T.C. Siegel, W.M. NeSmith, P.E. Cargill, C. City, presented at the 32nd DFI Annual Conference, Colorado Springs, CO 2007, pp. 1-8.
- [5] M.F. Randolph, J.P. Carter, C.P. Wroth, "Driven Piles in clay—The Effects of Installation and Subsequent Consolidation", *Geotechnique*, 1979, vol. 29, no. 4, pp. 361–393; DOI: [10.1680/geot.1979.29.4.361](https://doi.org/10.1680/geot.1979.29.4.361).
- [6] R.R. al-Omari, M.Y. Fattah, A.M. Kallawi, "Stress transfer from pile group in saturated and unsaturated soil using theoretical and experimental approaches", *MATEC Web Conference*, 2017, vol. 120, art. ID 06005, pp. 1-12; DOI: [10.1051/mateconf/201712006005](https://doi.org/10.1051/mateconf/201712006005).



- [7] J.H. Lee, R. Salgado, "Determination of Pile Base Resistance in Sands", *Journal of Geotechnical and Geoenvironmental Engineering*, 1999, vol. 125, no. 8, pp. 673–683; DOI: [10.1061/\(ASCE\)1090-0241\(1999\)125:8\(673\)](https://doi.org/10.1061/(ASCE)1090-0241(1999)125:8(673)).
- [8] Z.X. Yang, R.J. Jardine, B.T. Zhu, S. Rimoy, "Stresses Developed around Displacement Piles Penetration in Sand", *Journal of Geotechnical and Geoenvironmental Engineering*, 2014, vol. 140, no. 3, art. ID 04013027; DOI: [10.1061/\(ASCE\)GT.1943-5606.0001022](https://doi.org/10.1061/(ASCE)GT.1943-5606.0001022).
- [9] S. Fan, B. Bienen, M.F. Randolph, "Effects of Monopile Installation on Subsequent Lateral Response in Sand. II: Lateral Loading", *Journal of Geotechnical Geoenvironmental Engineering*, 2021, vol. 147, no. 5, art. ID 04021022; DOI: [10.1061/\(ASCE\)GT.1943-5606.0002504](https://doi.org/10.1061/(ASCE)GT.1943-5606.0002504).
- [10] S. Henke, J. Grabe, "Numerical investigation of soil plugging inside open-ended piles with respect to the installation method", *Acta Geotechnica*, 2008, vol. 3, no. 3, pp. 215–223; DOI: [10.1007/s11440-008-0079-7](https://doi.org/10.1007/s11440-008-0079-7).
- [11] K. Żarkiewicz, W. Qatameez, "Assessment of Stress in the Soil Surrounding the Axially Loaded Model Pile by Thin, Flexible Sensors", *Sensors*, 2021, vol. 21, no. 21, art. ID 7214; DOI: [10.3390/s21217214](https://doi.org/10.3390/s21217214).
- [12] B.M. Lehane, R.J. Jardine, A.J. Bond, R. Frank, "Mechanisms of Shaft Friction in Sand from Instrumented Pile Tests", *Journal of Geotechnical Engineering*, 1993, vol. 119, no. 1, pp. 19–35; DOI: [10.1061/\(ASCE\)0733-9410\(1993\)119:1\(19\)](https://doi.org/10.1061/(ASCE)0733-9410(1993)119:1(19)).
- [13] F. Burali d'Arezzo, S. Haigh, M. Talesnick, Y. Ishihara, "Measuring horizontal stresses during jacked pile installation", *Proceedings of the Institution of Civil Engineers - Geotechnical Engineering*, 2015, vol. 168, no. 4, pp. 306–318; DOI: [10.1680/geng.14.00069](https://doi.org/10.1680/geng.14.00069).
- [14] R.J. Jardine, B.T. Zhu, P. Foray, Z.X. Yang, "Measurement of stresses around closed-ended displacement piles in sand", *Géotechnique*, 2013, vol. 63, no. 1, pp. 1–17; DOI: [10.1680/geot.9.P.137](https://doi.org/10.1680/geot.9.P.137).
- [15] J.M.O. Hughes, P.K. Robertson, "Full-displacement pressuremeter testing in sand", *Canadian Geotechnical Journal*, 1985, vol. 22, no. 3, pp. 298–307; DOI: [10.1139/t85-043](https://doi.org/10.1139/t85-043).
- [16] E.I. Robinsky, C.F. Morrison, "Sand Displacement and Compaction around Model Friction Piles", *Canadian Geotechnical Journal*, 1964, vol. 1, no. 2, pp. 81–93; DOI: [10.1139/t64-002](https://doi.org/10.1139/t64-002).
- [17] R. Alsirawan, "Analysis of Embankment Supported by Rigid Inclusions Using Plaxis 3D", *Acta Technica Jaurinensis*, 2021, vol. 14, no. 4, pp. 455–476; DOI: [10.14513/actatechjaur.00615](https://doi.org/10.14513/actatechjaur.00615).
- [18] N. Linh, N. Nguyen, K. Nguyen, D. Nguyen, "Weighted dual approach to an equivalent stiffness-based load transfer model for jacked open-ended pile", *Journal of Applied and Computational Mechanics*, 2021, vol. 7, no. 3; DOI: [10.22055/jacm.2021.37430.3013](https://doi.org/10.22055/jacm.2021.37430.3013).
- [19] A. Shelke, N.R. Patra, "Effect of Arching on Uplift Capacity of Single Piles", *Geotechnical and Geological Engineering*, 2009, vol. 27, no. 3, pp. 365–377; DOI: [10.1007/s10706-008-9236-x](https://doi.org/10.1007/s10706-008-9236-x).
- [20] A.J. Bond, R.J. Jardine, "Effects of installing displacement piles in a high OCR clay", *Géotechnique*, 1991, vol. 41, no. 3, pp. 341–363; DOI: [10.1680/geot.1991.41.3.341](https://doi.org/10.1680/geot.1991.41.3.341).
- [21] B.M. Lehane, D.J. White, "Lateral stress changes and shaft friction for model displacement piles in sand", *Canadian Geotechnical Journal*, 2005, vol. 42, no. 4, pp. 1039–1052; DOI: [10.1139/t05-023](https://doi.org/10.1139/t05-023).
- [22] A.B. Lundberg, J. Dijkstra, F. van Tol, "On the modelling of piles in sand in the small geotechnical centrifuge", in *Eurofuge 2012*. Delft University of Technology and Deltares, 2012, p. 10.
- [23] J. Otani, K. Pham, J. Sano, "Investigation of Failure Patterns in Sand Due to Laterally Loaded Pile Using X-Ray CT", *Soils and Foundations*, 2006, vol. 46, no. 4, pp. 529–535; DOI: [10.3208/sandf.46.529](https://doi.org/10.3208/sandf.46.529).
- [24] B. Yuan, R. Chen, J. Teng, et al., "Investigation on 3D ground deformation and response of active and passive piles in loose sand", *Environmental Earth Sciences*, 2015, vol. 73, no. 11, pp. 7641–7649; DOI: [10.1007/s12665-014-3935-9](https://doi.org/10.1007/s12665-014-3935-9).
- [25] D. White, A. Take, M. Bolton, "Measuring soil deformation in geotechnical models using digital images and PIV analysis", in *10th International Conference Computer Methods and Advances Geomechanics*. CRC Press, 2001, pp. 997–1002.
- [26] Z.H. Cao, G.Q. Kong, H.L. Liu, H. Zhou, "Model test on deformation characteristic of pile driving in sand using piv technique", *Gongcheng Lixue/Engineering Mechanics*, 2014, vol. 31, no. 8, pp. 168–174; DOI: [10.6052/j.issn.1000-4750.2013.03.0217](https://doi.org/10.6052/j.issn.1000-4750.2013.03.0217).

- [27] A. Beijer-Lundberg, “Displacement pile installation effects in san”, Ph.D. thesis Delft University of Technology, 2015; DOI: [10.4233/UUID:01D8943F-E3EB-4051-8B44-32097E18C4DA](https://doi.org/10.4233/UUID:01D8943F-E3EB-4051-8B44-32097E18C4DA).
- [28] J. Dijkstra, W. Broere, O.M. Heeres, “Numerical simulation of pile installation”, *Computers and Geotechnics*, 2011, vol. 38, no. 5, pp. 612–622; DOI: [10.1016/j.compgeo.2011.04.004](https://doi.org/10.1016/j.compgeo.2011.04.004).
- [29] A.A. Al-Karni, “Shear Strength Reduction Due to Excess Pore Water Pressure”, in *Fourth International Conference on Recent Advances in Geotechnical Earthquake Engineering and Soil Dynamics*. 2001, pp. 1-7.
- [30] J. Dou, J. Chen, C. Liao, et al., “Study on the Correlation between Soil Consolidation and Pile Set-Up Considering Pile Installation Effect”, *Journal of Marine Science and Engineering*, 2021, vol. 9, no. 7, art. ID 705; DOI: [10.3390/jmse9070705](https://doi.org/10.3390/jmse9070705).
- [31] Y. Wang, X. Liu, M. Zhang, et al., “Field Test of Excess Pore Water Pressure at Pile–Soil Interface Caused by PHC Pipe Pile Penetration Based on Silicon Piezoresistive Sensor”, *Sensors*, 2020, vol. 20, no. 10, art. ID 2829; DOI: [10.3390/s20102829](https://doi.org/10.3390/s20102829).
- [32] K.Y. Lo, A.G. Stermac, “Induced pore pressures during pile-driving operations” in *6th International Conference on Soil Mechanics and Foundation Engineering (Montréal)*. 1965, pp. 1-6.
- [33] A. Wada, “Excess pore water pressure and its impact”, *Japanese Geotechnical Society Special Publication*, 2016, vol. 2, no. 7, pp. 335–339; DOI: [10.3208/jgssp.SEA-16](https://doi.org/10.3208/jgssp.SEA-16).
- [34] J.-H. Hwang, N. Liang, C.-H. Chen, “Ground Response during Pile Driving”, *Journal of Geotechnical and Geoenvironmental Engineering*, 2001, vol. 127, no. 11, pp. 939–949; DOI: [10.1061/\(asce\)1090-0241\(2001\)127:11\(939\)](https://doi.org/10.1061/(asce)1090-0241(2001)127:11(939)).
- [35] M.Y. Fattah, F.S. Mustafa, “Development of Excess Pore Water Pressure around Piles Excited by Pure Vertical Vibration”, *International Journal of Civil Engineering*, 2017, vol. 15, no. 6, pp. 907–920; DOI: [10.1007/s40999-016-0073-7](https://doi.org/10.1007/s40999-016-0073-7).
- [36] K.D. Eigenbrod, T. Issigonis, “Pore-water pressures in soft to firm clay during driving of piles into underlying dense sand”, *Canadian Geotechnical Journal*, 1996, vol. 33, no. 2, pp. 209–218; DOI: [10.1139/t96-001](https://doi.org/10.1139/t96-001).
- [37] R.D. Holtz, P. Boman, “A New Technique for Reduction of Excess Pore Pressures During Pile Driving”, *Canadian Geotechnical Journal*, 1974, vol. 11, no. 3, pp. 423–430; DOI: [10.1139/t74-043](https://doi.org/10.1139/t74-043).
- [38] J.M. Pestana, C.E. Hunt, J.D. Bray, “Soil Deformation and Excess Pore Pressure Field around a Closed-Ended Pile”, *Journal of Geotechnical and Geoenvironmental Engineering*, 2002, vol. 128, no. 1, pp. 1–12; DOI: [10.1061/\(ASCE\)1090-0241\(2002\)128:1\(1\)](https://doi.org/10.1061/(ASCE)1090-0241(2002)128:1(1)).
- [39] M.S. Nataraja, B.E. Cook, “Increase in SPT N-values due to displacement piles”, *Journal of Geotechnical Engineering*, 1986, vol. 112, no. 10, pp. 969–971; DOI: [10.1061/\(ASCE\)0733-9410\(1986\)112:10\(969\)](https://doi.org/10.1061/(ASCE)0733-9410(1986)112:10(969)).
- [40] T.C. Siegel, W.M. NeSmith, W.M. NeSmith, P.E. Cargill, “Ground improvement resulting from installation of drilled displacement piles”, in *Proceedings of the DFI's 32nd Annual Conference Deep Foundations*. Colorado Springs, USA, 2007, pp. 129–138.
- [41] A.W. Stuedlein, T.N. Gianella, G. Canivan, “Densification of Granular Soils Using Conventional and Drained Timber Displacement Piles”, *Journal of Geotechnical and Geoenvironmental Engineering*, 2016, vol. 142, no. 12; DOI: [10.1061/\(asce\)gt.1943-5606.0001554](https://doi.org/10.1061/(asce)gt.1943-5606.0001554).
- [42] G.G. Meyerhof, “Compaction of Sands and Bearing Capacity of Piles”, *Journal of the Soil Mechanics and Foundations Division*, 1959, vol. 85, no. 6, pp. 1–29; DOI: [10.1061/jsfeaq.0000231](https://doi.org/10.1061/jsfeaq.0000231).
- [43] C. Szechy, “The Effects of Vibration and Driving Upon the Voids in Granular Soil Surrounding a Pile”, in *Soil Mechanics and Foundation Engineering*, vol. 2. 1961, pp. 61–164.
- [44] H. Kishida, “Ultimate Bearing Capacity of Piles Driven into Loose Sand”, *Soils and Foundations*, 1967, vol. 7, no. 3, pp. 20–29; DOI: [10.3208/sandf1960.7.3_20](https://doi.org/10.3208/sandf1960.7.3_20).
- [45] K. Terzaghi, R.B. Peck, G. Mesri, *Soil Mechanics in Engineering Practice*. John Wiley & Sons, 1996.
- [46] N. Barounis, J. Philpot, “Designing timber compaction piles to achieve a target soil density using CPTu data”, presented at NZGS Symposium 2021, New Zealand, pp. 1-8.
- [47] A. Krasieński, “Advanced Field Investigations of Screw Piles and Columns”, *Archives of Civil Engineering*, 2011, vol. 57, no. 1, pp. 45–57; DOI: [10.2478/v.10169-011-0005-5](https://doi.org/10.2478/v.10169-011-0005-5).



- [48] M.Y. Abu-Farsakh, Md. N. Haque, C. Tsai, "A full-scale field study for performance evaluation of axially loaded large-diameter cylinder piles with pipe piles and PSC piles", *Acta Geotechnica*, 2017, vol. 12, no. 4, pp. 753–772; DOI: [10.1007/s11440-016-0498-9](https://doi.org/10.1007/s11440-016-0498-9).
- [49] L.C. Hung, T.D. Nguyen, J.-H. Lee, S.-R. Kim, "Applicability of CPT-based methods in predicting toe bearing capacities of driven piles in sand", *Acta Geotechnica*, 2016, vol. 11, no. 2, pp. 359–372; DOI: [10.1007/s11440-015-0398-4](https://doi.org/10.1007/s11440-015-0398-4).
- [50] R. Munro, "International Society for Soil Mechanics and Geotechnical Engineering (ISSMGE)", in *Encyclopedia of Engineering Geology*, P.T. Bobrowsky, B. Marker, Eds. Cham: Springer International Publishing, 2018, pp. 536–537; DOI: [10.1007/978-3-319-73568-9_174](https://doi.org/10.1007/978-3-319-73568-9_174).
- [51] H. Peiffer, W. Van Impe, G. Cortvrindt, M. Bottiau, "Evaluation of the influence of pile execution parameters on the soil condition around the pile shaft of a PSC-pile", in *Deep Foundations on Bored & Auger Piles : Bap II*, vol. 1. AA Balkema, 1993, pp. 217–220.
- [52] I. Van, H. Peiffer, "Evaluation of pile performance based on soil stress measurements - Field test program", in *Deep Foundations on Bored & Auger Piles : Bap II*, vol. 1. AA Balkema, 1993, pp. 385–389.
- [53] S. Amoroso, et al., "Comparative Study of CPTU and SDMT in Liquefaction-Prone Silty Sands with Ground Improvement", *Journal of Geotechnical and Geoenvironmental Engineering*, 2022, vol. 148, no. 6, art. ID 04022038; DOI: [10.1061/\(ASCE\)GT.1943-5606.0002801](https://doi.org/10.1061/(ASCE)GT.1943-5606.0002801).
- [54] P. Monaco, D. Marchetti, "Evaluation of OCR in sand from DMT & CPT", 2017, pp. 1–15.
- [55] A.W. Stuedlein, T.N. Gianella, G. Canivan, "Densification of Granular Soils Using Conventional and Drained Timber Displacement Piles", *Journal of Geotechnical and Geoenvironmental Engineering*, 2016, vol. 142, no. 12, art. ID 04016075; DOI: [10.1061/\(asce\)gt.1943-5606.0001554](https://doi.org/10.1061/(asce)gt.1943-5606.0001554).
- [56] S. Lobo-Guerrero, L.E. Vallejo, "Influence of pile shape and pile interaction on the crushable behavior of granular materials around driven piles: DEM analyses", *Granular Matter*, 2007, vol. 9, no. 3–4, pp. 241–250; DOI: [10.1007/s10035-007-0037-3](https://doi.org/10.1007/s10035-007-0037-3).
- [57] Y. Lv, H. Liu, X. Ding, G. Kong, "Field Tests on Bearing Characteristics of X-Section Pile Composite Foundation", *Journal of Performance of Constructed Facilities*, 2012, vol. 26, no. 2, pp. 180–189; DOI: [10.1061/\(ASCE\)CF.1943-5509.0000247](https://doi.org/10.1061/(ASCE)CF.1943-5509.0000247).
- [58] M. Ghazavi, "Experimental Analysis of Ground Vibration Due to Tapered Piles Driving", presented at 7th International Conference on Seismology and Earthquake Engineering, Iran, 2015.
- [59] M.K. Khan, M.H. El Naggar, M. Elkasabgy, "Compression testing and analysis of drilled concrete tapered piles in cohesive-frictional soil", *Canadian Geotechnical Journal*, 2008, vol. 45, no. 3, pp. 377–392; DOI: [10.1139/T07-107](https://doi.org/10.1139/T07-107).
- [60] W. Wu, G. Jiang, B. Dou, C.J. Leo, "Vertical Dynamic Impedance of Tapered Pile considering Compacting Effect", *Mathematical Problems in Engineering*, 2013, vol. 2013, pp. 1–9; DOI: [10.1155/2013/304856](https://doi.org/10.1155/2013/304856).
- [61] J. Liu, J. He, Y.-P. Wu, Q.-G. Yang, "Load transfer behaviour of a tapered rigid pile", *Géotechnique*, 2012, vol. 62, no. 7, pp. 649–652; DOI: [10.1680/geot.11.T.001](https://doi.org/10.1680/geot.11.T.001).
- [62] M. Sakr, M.H. El Naggar, M. Nehdi, "Lateral behaviour of composite tapered piles in dense sand", *Proceedings of the Institution of Civil Engineers - Geotechnical Engineering*, 2005, vol. 158, no. 3, pp. 145–157; DOI: [10.1680/geng.2005.158.3.145](https://doi.org/10.1680/geng.2005.158.3.145).
- [63] R. Butterfield, P.K. Banerjee, "The Elastic Analysis of Compressible Piles and Pile Groups", *Géotechnique*, 1971, vol. 21, no. 1, pp. 43–60; DOI: [10.1680/geot.1971.21.1.43](https://doi.org/10.1680/geot.1971.21.1.43).
- [64] M. Sakr, M. Hesham El Naggar, "Centrifuge Modeling of Tapered Piles in Sand", *Geotechnical Testing Journal*, 2003, vol. 26, no. 1; DOI: [10.1520/GTJ11106J](https://doi.org/10.1520/GTJ11106J).
- [65] J. Wei, M.H. El Naggar, "Experimental study of axial behaviour of tapered piles", *Canadian Geotechnical Journal*, 1998, vol. 35, no. 4, pp. 641–654; DOI: [10.1139/t98-033](https://doi.org/10.1139/t98-033).
- [66] S.D. Zil'berberg, A.D. Sherstnev, "Construction of compaction tapered pile foundations (from the experience of the "Vladspetsstroj" trust)", *Soil Mechanics and Foundation Engineering*, 1990, vol. 27, no. 3, pp. 96–101; DOI: [10.1007/BF02306664](https://doi.org/10.1007/BF02306664).
- [67] A.W. Stuedlein, T.N. Gianella, "Effects of Driving Sequence and Spacing on Displacement-Pile Capacity", *Journal of Geotechnical and Geoenvironmental Engineering*, 2017, vol. 143, no. 3, art. ID 06016026; DOI: [10.1061/\(ASCE\)GT.1943-5606.0001618](https://doi.org/10.1061/(ASCE)GT.1943-5606.0001618).



- [68] F. Chow, “Field measurements of stress interactions between displacement piles in sand”, *International Journal of Rock Mechanics and Mining Sciences & Geomechanics Abstracts*, 1996, vol. 33, no. 2; DOI: [10.1016/0148-9062\(96\)84051-4](https://doi.org/10.1016/0148-9062(96)84051-4).
- [69] A. Le Kouby, J.C. Dupla, J. Canou, R. Francis, “The effects of installation order on the response of a pile group in silica sand”, *Soils Foundations*, 2016, vol. 56, no. 2, pp. 174–188; DOI: [10.1016/j.sandf.2016.02.002](https://doi.org/10.1016/j.sandf.2016.02.002).

Received: 2022-05-09, Revised: 2022-07-22